J. Fluid Mech. (2010), *vol.* 657, *pp.* 22–35. © Cambridge University Press 2010
doi:10.1017/S0022112010001291

Impact of a falling jet

PAUL CHRISTODOULIDES[1] AND FRÉDÉRIC DIAS[2,3]†

[1]Faculty of Engineering and Technology, Cyprus University of Technology, Limassol, Cyprus

[2]CMLA, ENS Cachan and CNRS, UniverSud, 61 avenue du President Wilson, F-94235 Cachan cedex, France

[3]School of Mathematical Sciences, University College Dublin, Belfield, Dublin 4, Ireland

(Received 9 December 2009; revised 9 March 2010; accepted 9 March 2010; first published online 6 July 2010)

Given the complexity of the problem of the impact of a mass of liquid on a solid structure, various simplified models have been introduced in order to obtain some insight on particular aspects of the problem. Here the steady flow of a jet falling from a vertical pipe, hitting a horizontal plate and flowing sideways is considered. Depending on the elevation H of the pipe relative to the horizontal plate and the Froude number F, the flow can either leave the pipe tangentially or detach from the edge of the pipe. When the flow leaves tangentially, it can either be diverted immediately by the plate or experience squeezing before being diverted. First, the problem is reformulated using conformal mappings. The resulting problem is then solved by a collocation Galerkin method; a particular form is assumed for the solution, and certain coefficients in that representation are then found numerically by satisfying Bernoulli's equation on the free surfaces at certain discrete points. The resulting equations are solved by Newton's method, yielding various configurations of the solution based on the values of F and H. The pressure exerted on the plate is computed and discussed. For a fixed value of F, the maximum pressure along the plate goes through a minimum as H increases from small to large values. Results are presented for the three possible configurations: (i) tangential departure from the pipe and no squeezing, (ii) tangential departure from the pipe followed by squeezing of the liquid and (iii) detachment of the liquid from the pipe (with subsequent squeezing).

1. Introduction

The problem of a jet impacting on a wall is a fascinating one, with very practical applications. Indeed the impact of a fluid on a structure often occurs as a mass of liquid pushing the gas around it and hitting the solid structure ahead. It is a quite challenging fluid mechanics problem as suggested by some of its features, such as the nonlinearity of its free surface, the possible presence and importance of the compressibility effects when gas is trapped by the fluid, the role of the possible elasticity of its structure. A description of all phenomena which can take place when a jet hits a structure can be found in Braeunig *et al.* (2009). Before making an attempt to consider all the effects together, it is important to understand each effect separately. Various studies involving incompressible flows have been performed by Garabedian (1957), Birkhoff & Carter (1957), Vanden-Broeck (1984, 1986, 1991), Modi (1985)

† Email address for correspondence: dias@cmla.ens-cachan.fr

https://doi.org/10.1017/S0022112010001291 Published online by Cambridge University Press

and Christodoulides & Dias (2009). Various aspects of compressibility have been considered by Peregrine & Thais (1996) and Braeunig *et al.* (2010).

The simpler problem of a falling jet without horizontal plate has led to several papers. The main motivation was the study of a long bubble rising through an infinite plane vertical tube of liquid. This problem can be actually viewed – if one uses a co-ordinate system attached to the bubble – as a liquid falling around a bubble, instead of the bubble rising in the liquid. A variation of this problem is that of jets falling from nozzles and funnels (Lee & Vanden-Broeck 1993, 1998) and that of bubbles rising in an inclined pipe (Couët & Strumolo 1987; Inogamov & Oparin 2003). Other variations are the emptying or the filling of a closed pipe, the flow from a vertical slot into a fluid layer or from a fluid layer into a vertical slot, and surf-skimmer planing hydrodynamics (Benjamin 1968; Tuck & Dixon 1989; Hocking 1992; Korobkin 1995; Merino 1996; Peregrine & Kalliadassis 1996; Michallet *et al.* 2001). In these problems, one often has an infinite solid boundary on one side and a semi-infinite solid boundary on the other side from which a free surface detaches. The reversed problem in which a horizontal jet hits a vertical wall has been considered by Dias & Tuck (1993).

In this paper, we provide a better understanding of the incompressible flow impacting on a solid plate. Comments on compressible aspects will be given at the end of the paper. A stream of fluid flows down and out of the bottom of a long two-dimensional vertically-sided pipe of half-width W. The downwardly directed flow meets a horizontal plate of infinite extent set at a distance H below the bottom end of the pipe. The flow splits into two jets on each side of the pipe following a path along the horizontal plate. The solution depends on the ratio H/W and the dimensionless Froude number,

$$F = \frac{U}{\sqrt{gW}}, \tag{1.1}$$

where g is the acceleration due to gravity and U is the velocity of the fluid far inside the pipe. Because compressible effects are neglected here, the Mach number $M = U/c$, where c is the speed of sound, does not come into the picture. In other words, we consider the limit $M = 0$.

The main results of the present study are twofold. There are three regions in the $(F, H/W)$ plane, shown in figure 1. These regions are divided by two curves, which are found numerically. In region I, the jet emerges from the pipe without a stagnation point and is immediately deflected. In region II, the jet emerges from the pipe without a stagnation point but experiences squeezing before being deflected by the horizontal plate. In region III, the jet emerges from the pipe with a stagnation point.

In § 2, applying the theory of functions of complex variables and conformal mappings leads to a formulation of the problem that is well-suited for discretization. A system of N nonlinear equations in N unknowns is then derived and the problem is solved numerically through a collocation Galerkin method explained in § 3. Section 3 provides the numerical results and some computed profiles of the free surfaces are presented. In § 4 we study related flows where the detachment point along the plate is a stagnation point. A study of the pressure along the horizontal plate is performed in § 5. For a fixed value of F, the maximum pressure along the plate goes through a minimum as H increases. It is shown that for small values of H the pressure behaves like $1/H^2$, while for large values of H it is proportional to H. The various physical phenomena that have been neglected in the present study are discussed in § 6. These include asymmetry, compressibility and three-dimensional effects.

https://doi.org/10.1017/S0022112010001291 Published online by Cambridge University Press

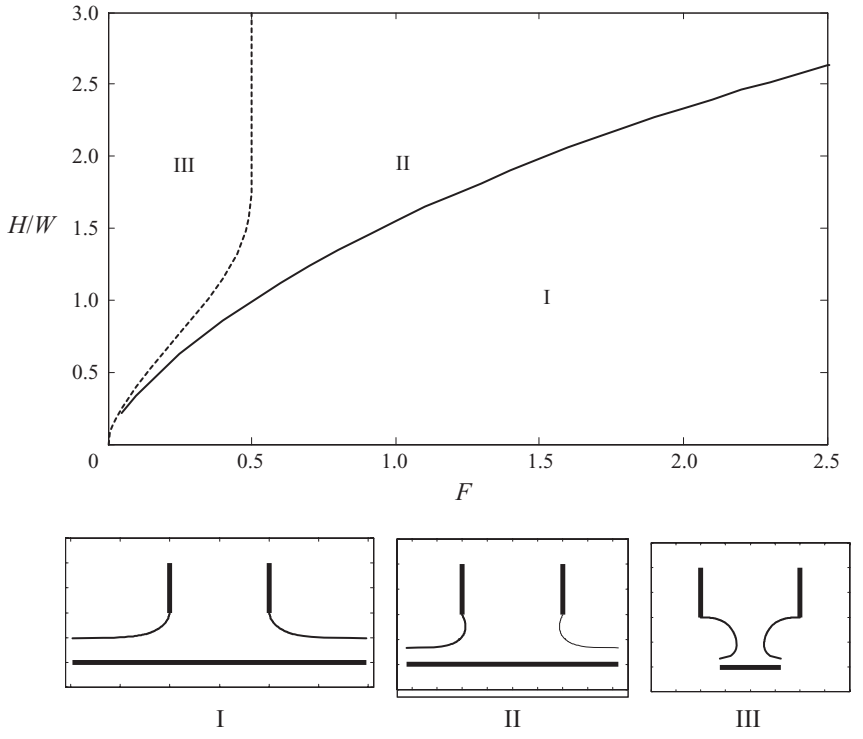


FIGURE 1. The falling jets considered in this paper depend on two parameters: the Froude number F and the aspect ratio between the falling altitude and the pipe width H/W. The two plotted curves divide the $(F, H/W)$ plane into three regions. In region I, the jet emerges from the pipe without a stagnation point and is immediately deflected. In region II, the jet emerges from the pipe without a stagnation point but experiences squeezing before being deflected by the horizontal plate. In region III, the jet emerges from the pipe with a stagnation point. Solutions of types I and II have 180° contact angle, solutions of type III have 90° contact angle, while solutions with 120° contact angle appear on the II/III border.

2. Formulation of the problem

We consider the steady irrotational flow of an incompressible inviscid fluid falling from a pipe of width $2W$ under gravity, hitting a horizontal plate of infinite length placed at a vertical distance H from the bottom edges of the pipe and splitting symmetrically into two jets one on each side of the pipe. As shown in figure 2(a), the stream coming from far inside the pipe (see points J, J') hits the horizontal plate, centered at point C, and forms two jets – one on each side – detaching at points A, A' and forming free surfaces $A \to I$, $A' \to I'$.

Because of symmetry, the formulation of the problem is based on the 'right' half of the flow. The results presented in the sequel are simply obtained by superposition of the 'left' and 'right' flows. The point A is taken as the origin of the coordinate system (x, y), x being horizontal and y vertical. The mass flux emerging from the 'right' pipe is

$$Q = UW. \tag{2.1}$$

As the system is governed by the assumptions of irrotationality and incompressibility, we have $(u, v) = \nabla\phi$, u and v being the x- and y-components of the fluid velocity, with Laplace's equation $\nabla^2\phi = 0$ holding for the velocity potential ϕ. Bernoulli's

https://doi.org/10.1017/S0022112010001291 Published online by Cambridge University Press

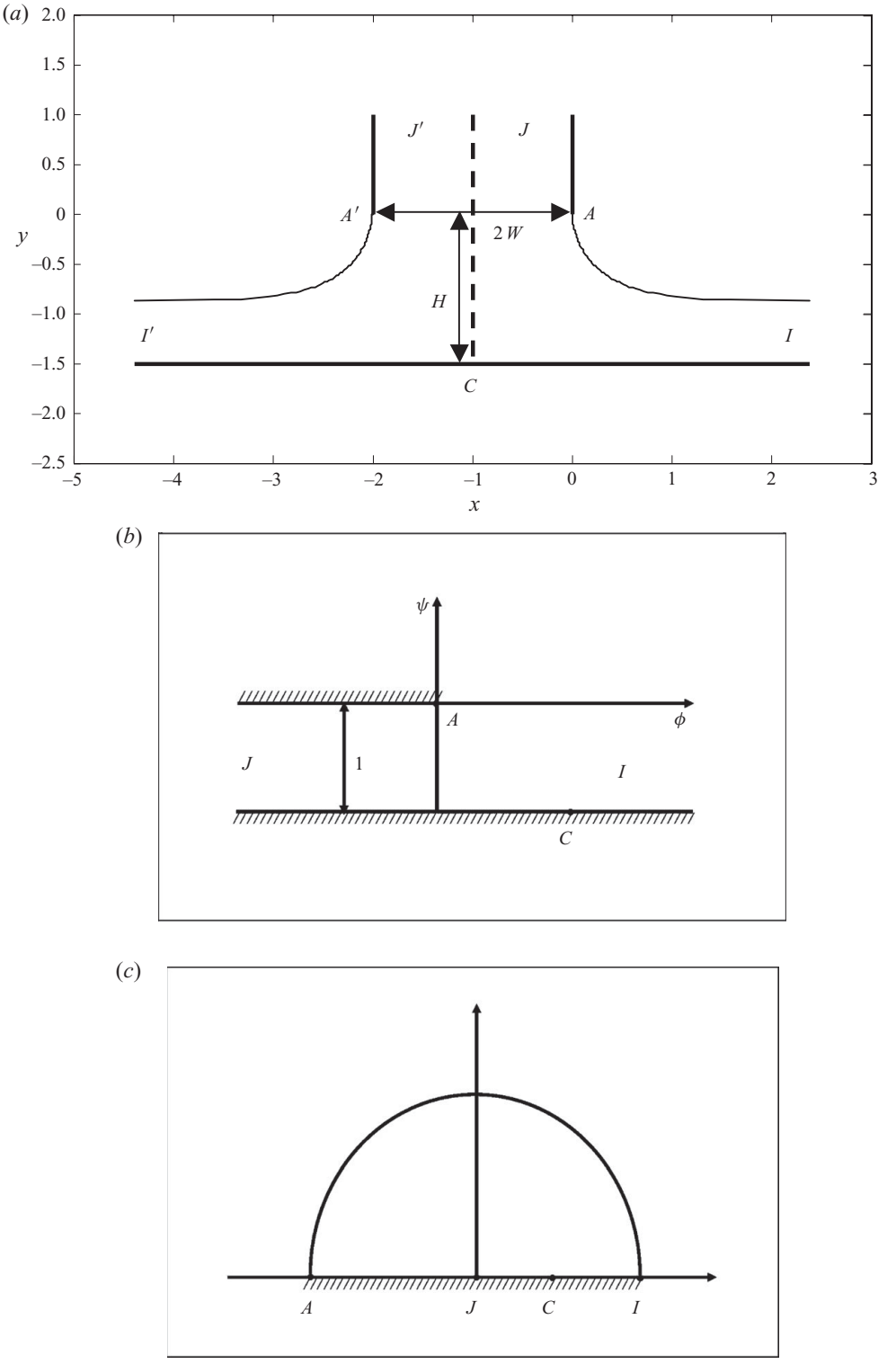


FIGURE 2. (*a*) Sketch of the flow and the coordinates. The free-surface profile is a computed solution for $H = 1.5$ and $F = 1.5$. Special points are labelled on the boundary. (*b*) The complex potential f-plane with the images of the special points. (*c*) The complex t-plane with the images of the special points.

https://doi.org/10.1017/S0022112010001291 Published online by Cambridge University Press

equation follows as a first integral of the Euler (momentum) equations of motion, is valid everywhere inside the fluid and reads

$$\frac{1}{2}(u^2+v^2)+gy+\frac{p}{\rho}=\text{constant}, \tag{2.2}$$

where p is the pressure and ρ is the fluid density. Assuming a zero pressure on all free surfaces, and taking W and U as the unit length and unit velocity, respectively, and consequently Q becoming unity, Bernoulli's equation on the free surfaces becomes, in dimensionless form,

$$\frac{1}{2}(u^2+v^2)+\frac{1}{F^2}y=\frac{1}{2}v_A^2, \tag{2.3}$$

where the same symbols are kept for the dimensionless variables for the sake of simplicity. The constant on the right-hand side has been evaluated at point A, where the velocity is purely vertical and $y=0$.

The problem under consideration can be solved with the use of conformal mappings. Hence, we can define the complex variable $z=x+\mathrm{i}y$ and the complex potential $f=\phi+\mathrm{i}\psi$, for the velocity potential $\phi(x,y)$ and the streamfunction $\psi(x,y)$, and the hodograph variable

$$\zeta(z)\equiv\frac{\mathrm{d}f}{\mathrm{d}z}=u-\mathrm{i}v, \tag{2.4}$$

which is the conjugate complex velocity and is an analytic function of z. The flow domain in the f-plane is represented in figure 2(b). It lies within an infinite strip of height 1. Without loss of generality, the point A is taken as the origin of the complex potential. Following Tuck & Vanden-Broeck (1984) and Hocking (1985), the domain of the fluid in the f-plane is then transformed into the upper half of the unit disk in the t-plane so that points A, J and I are mapped into points -1, 0 and 1, respectively, as shown in figure 2(c). The solid boundaries are mapped into the real diameter of the unit circle $t\in[-1,1]$. The 'left' side of the half-pipe goes onto $[0,t_C]$, the right side onto $[-1,0]$, while the horizontal plate goes onto $[t_C,1]$, with the free surface going onto the half-circle. The transformation from the f-plane to the t-plane can be written in differential form as

$$\frac{\mathrm{d}f}{\mathrm{d}t}=\frac{1}{\pi}\frac{1+t}{t(1-t)} \tag{2.5}$$

or, in integrated form, as

$$f=\frac{1}{\pi}\ln\left(\frac{t}{(1-t)^2}\right). \tag{2.6}$$

It is clear that t can be obtained as a function of f explicitly by inverting relation (2.6).

The problem now reduces to finding the hodograph variable ζ as an analytic function of t, satisfying Bernoulli's equation (2.3) on the free surfaces and the following kinematic boundary condition on the real diameter $t\in[-1,1]$:

$$\mathrm{Re}(\zeta)=0 \quad \text{for } t\in[-1,t_C], \qquad \mathrm{Im}(\zeta)=0 \quad \text{for } t\in[t_C,1].$$

There is a singularity at point C, where the velocity of the fluid vanishes and the appropriate behaviour for ζ is given by

$$\zeta\sim(t-t_C)^{1/2} \quad \text{as} \quad t\to t_C. \tag{2.7}$$

https://doi.org/10.1017/S0022112010001291 Published online by Cambridge University Press

It is then possible to define ζ by the relation

$$\zeta(t) = \frac{(t - t_C)^{1/2}}{(t_C)^{1/2}} e^{\Omega(t)}, \tag{2.8}$$

where $\zeta(0) = i$ and the function $\Omega(t)$ is analytic for $|t| < 1$, continuous for $|t| \leqslant 1$, and can be expanded in a power series of the form

$$\Omega(t) = \sum_{n=1}^{\infty} a_n t^n. \tag{2.9}$$

Then, parametrizing the free surface in the t-plane by $t = e^{i\sigma}$, $\sigma \in [0, \pi]$, and differentiating Bernoulli's equation (2.3) with respect to σ yields

$$uu_\sigma + vv_\sigma + \frac{1}{\pi F^2} \left(\frac{\cos(\sigma/2)}{\sin(\sigma/2)} \right) \frac{u}{u^2 + v^2} = 0. \tag{2.10}$$

This completes the reformulation of the problem.

3. Numerical method and results

The coefficients a_n in the power series (2.9) are real and can be determined by using a collocation Galerkin method. We truncate the infinite series after N terms and introduce on the free surfaces the N mesh points

$$\sigma_M = \frac{\pi}{N} \left(M - \frac{1}{2} \right), \; M = 1, \ldots, N. \tag{3.1}$$

Substitution of the expression of ζ into (2.10) at the mesh points σ_M, yields N nonlinear algebraic equations for the N unknowns $a_1, \ldots, a_N$. Given the distance $H \in (0, \infty)$, this system is solved by Newton's method for given values of the Froude number $F \in (0, \infty)$, thus giving a two-parameter family of solutions.

All computations were performed in MATLAB and, unless otherwise stated, $N = 200$ mesh points were used for the computations presented in the sequel, after a check on accuracy was performed. Typical orders of magnitude for a_1, a_{20}, a_{100} are $|a_1| \approx 10^{-1}$, $|a_{20}| \approx 10^{-3}$, $|a_{100}| \approx 10^{-5}$, respectively.

In figure 2(*a*), we have shown a computed solution in which the distance of the horizontal plate from the end of the pipe is $H = 1.5$ (i.e. the H/W ratio is 1.5) for a relatively large value of the Froude number $F = 1.5$. One can see that the flow leaves the pipe at A (A') tangentially at an angle of 180° and gradually moves to the right (left) forming a single-free-surface jet that moves along the horizontal plate to $+\infty$ ($-\infty$). Keeping F fixed at 1.5 and letting H vary has the following effect in the behaviour of the flow. As shown in figure 3 for 'small' $H = 0.2$ the flow, after detaching, moves to the right (left) almost immediately and continues along the horizontal plate to $+\infty$ ($-\infty$). For 'large' $H = 3.0$ (see figure 4), the jet becomes thinner (i.e. the fluid is effectively being 'squeezed') after detaching, then is gradually diverted and finally moves along the horizontal plate to $+\infty$ ($-\infty$).

Increasing the Froude number to 'large' values has no effect on the behaviour of the flow for small to medium heights H. This behaviour, however, persists even for large values of H, as demonstrated in figure 5, where $F = 10$ and $H = 3.0$. One can observe that there is no squeezing of the free surfaces. In fact, for $H = 3.0$, the 'transition' value of F (separating the regions with and without squeezing) is 3.3.

https://doi.org/10.1017/S0022112010001291 Published online by Cambridge University Press

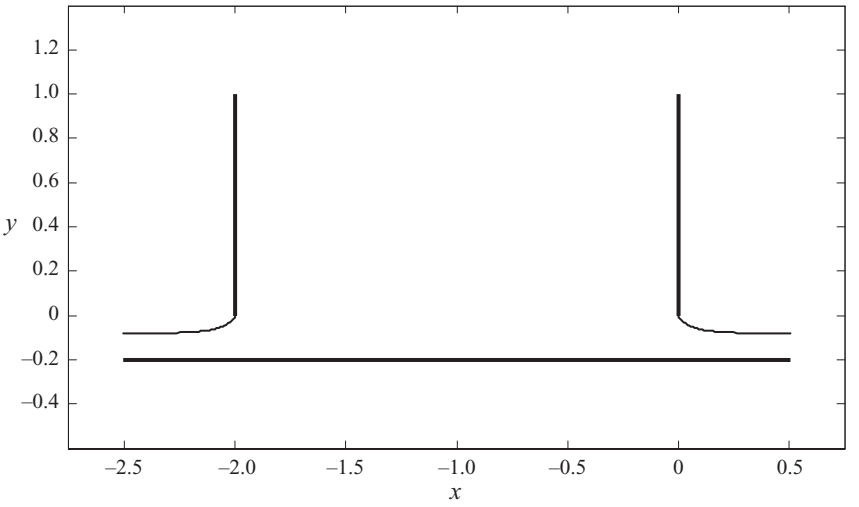


FIGURE 3. Free-surface profiles for parameter values $H = 0.2$ and $F = 1.5$.

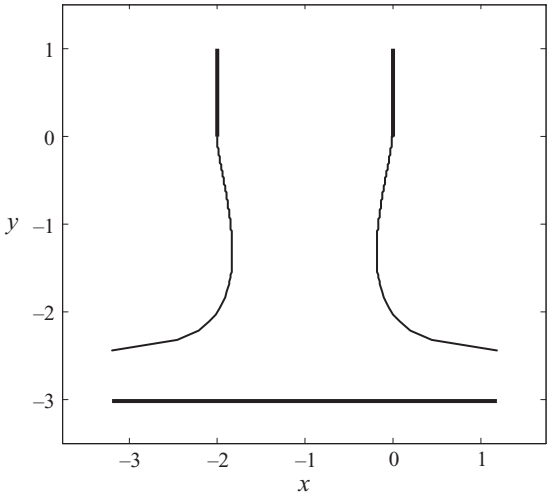


FIGURE 4. Free-surface profiles for parameter values $H = 3.0$ and $F = 1.5$ ($N = 400$).

The curve along which the transition between squeezing and no-squeezing occurs is shown in figure 1. It is the curve that separates region I from region II. Because of the shape of that boundary, it is clear that decreasing the Froude number leads to more and more values of the height H with the occurrence of the squeezing of the free surfaces. An example is shown in figure 6, where $F = 0.7$ and $H = 1.5$. In fact, for $H = 1.5$, the transition value of F (separating the regions with and without squeezing) is 0.93.

From the numerical point of view, it is sometimes tricky to distinguish between the two cases when the squeezing occurs very close to the end of the pipe. In § 5 we will indicate a more precise way to obtain the boundary between squeezing and no squeezing.

To summarize, we have so far found two types of flows: flows without squeezing in region I (these flows look relatively similar to the equivalent flow in the absence of

https://doi.org/10.1017/S0022112010001291 Published online by Cambridge University Press

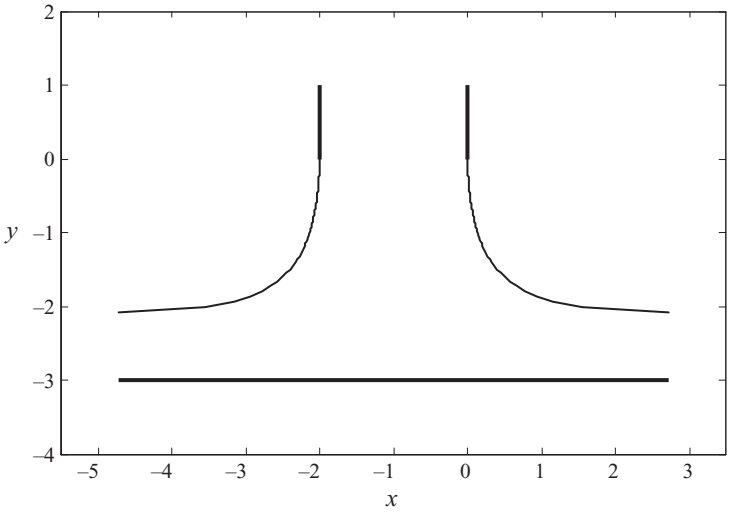


FIGURE 5. Free-surface profiles for parameter values $H = 3.0$ and $F = 10$.

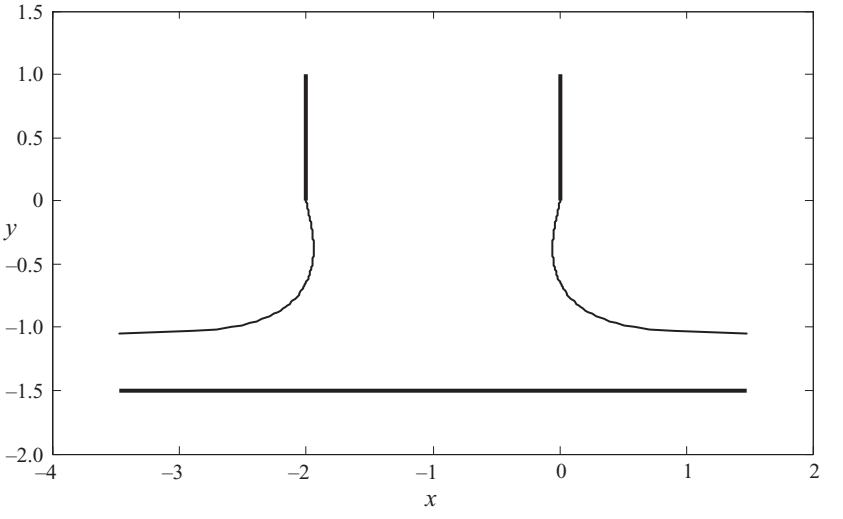


FIGURE 6. Free-surface profiles for parameter values $H = 1.5$ and $F = 0.7$.

gravity considered in the monograph by Milne-Thomson 1996, Example XII.10 and figure 14.8*b*) and flows with squeezing in region II (these flows are strongly influenced by gravity).

4. Flows with a stagnation point and other flows

If one wishes to impose the condition that the flow exhibits stagnation points at the ends of the pipes A and A', then – following the formulation in § 2 – there will be an extra singularity in the complex velocity, in addition to the singularity at point C defined in (2.7). As in the simplified configuration of a falling jet in the absence

https://doi.org/10.1017/S0022112010001291 Published online by Cambridge University Press

of the horizontal plate (Vanden-Broeck 1984, 1986), the only possible values for the angles between the vertical side of the pipe and the free surface are 90° and 120°. The 90° case corresponds to the free surface leaving the side of the pipe horizontally, while the 120° case corresponds to the free surface leaving the side of the pipe at a 60° angle from the vertical. The singularities are as follows:

$$\text{For a } 120^\circ \text{ stagnation point}, \quad \zeta \sim (t+1)^{2/3} \quad \text{as} \quad t \to -1, \tag{4.1a}$$

or

$$\text{for a } 90^\circ \text{ stagnation point}, \quad \zeta \sim t+1 \quad \text{as} \quad t \to -1. \tag{4.1b}$$

It is then possible to define the hodograph variable ζ, respectively, by the relations

$$\zeta(t) = \frac{(t+1)^{2/3}(t-t_C)^{1/2}}{(t_C)^{1/2}} \mathrm{e}^{\Omega(t)}, \tag{4.2a}$$

or

$$\zeta(t) = \frac{(t+1)(t-t_C)^{1/2}}{(t_C)^{1/2}} \mathrm{e}^{\Omega(t)}, \tag{4.2b}$$

where $\zeta(0) = \mathrm{i}$ and the function $\Omega(t)$, as before, is analytic for $|t| < 1$, continuous for $|t| \leqslant 1$, and can be expanded in a power series of the form (2.9).

For the 120° stagnation point, the numerical process follows a similar pattern to the one in § 3 with the difference that the infinite series is truncated after $N-1$ terms. The free surfaces are still described by N mesh points $\sigma_M = (\pi/N)(M - 1/2)$, $M = 1, \ldots, N$, and the system to be solved consists of N nonlinear algebraic equations in the N unknowns $a_1, \ldots, a_{N-1}$, F, thus giving a one-parameter ($H \in (0, \infty)$) family of solutions. Again, unless otherwise stated, $N = 200$ mesh points were used for most computations. Typical orders of magnitude for a_1, a_{20}, a_{100} are $|a_1| \approx 10^{-1}$, $|a_{20}| \approx 10^{-3}$, $|a_{100}| \approx 10^{-5}$, respectively.

It turns out that such flows exist only for 'small' Froude numbers, $F_s \leqslant 0.50 = F_c$. Actually, this critical value F_c corresponds exactly to the one found by Vanden-Broeck (1984) in his study of jets falling from a nozzle (note that by definition the Froude number of the present paper is equal to $\sqrt{2}$ times the Froude number in Vanden-Broeck's paper). Even though the critical value F_c is very close to 1/2, there is no obvious reason why it should be exactly 1/2. The present case of a vertical pipe is different from the case of a horizontal pipe. When the pipe is horizontal, the critical value for the Froude number is indeed exactly 1/2. The proof uses global conservation laws as well as Bernoulli's equation. This result was first proved by Benjamin (1968). Note also that in the horizontal case, solutions cease to exist when the Froude number drops below 1/2.

The curve that gives F_s as a function of the elevation H is given in figure 1. It is the boundary between regions II and III. As H increases, F_s approaches the limiting value of 0.5, which corresponds to the configuration in the absence of the horizontal plate. A typical flow is shown in figure 7 for $H = 1.01$, corresponding to a Froude number of $F = 0.35$. One can see that the flow detaches at A (A') at an angle of 120° and gradually turns to the right (left) and moves along the horizontal plate to $+\infty$ ($-\infty$). Note that the same results can be obtained through the formulation in § 3 but the convergence is not as good. The reason is that the singularity is so local that it does not affect much the rest of the solution. However, the main difference between the algorithm of § 3 and the algorithm here is the number of free parameters: two (F and H) previously (tangential case), only one (F or H) in the 120° case.

https://doi.org/10.1017/S0022112010001291 Published online by Cambridge University Press

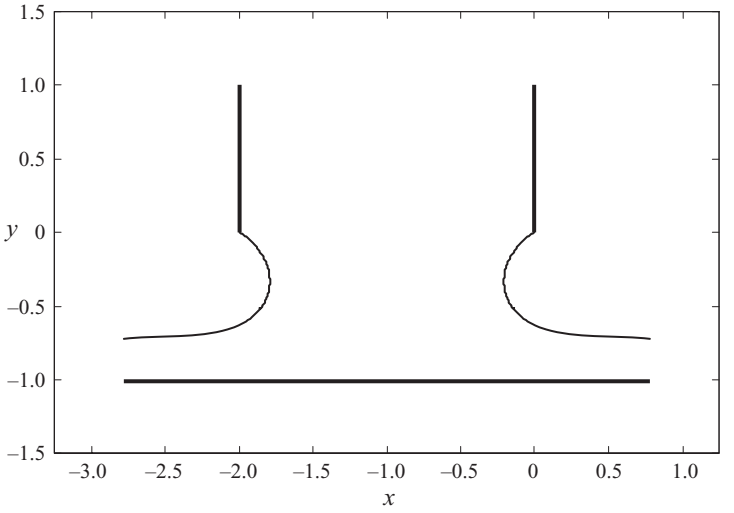


FIGURE 7. Free-surface profiles with 120° stagnation points at A, A' for $H = 1.01$. The Froude number $F = 0.35$ comes as part of the solution.

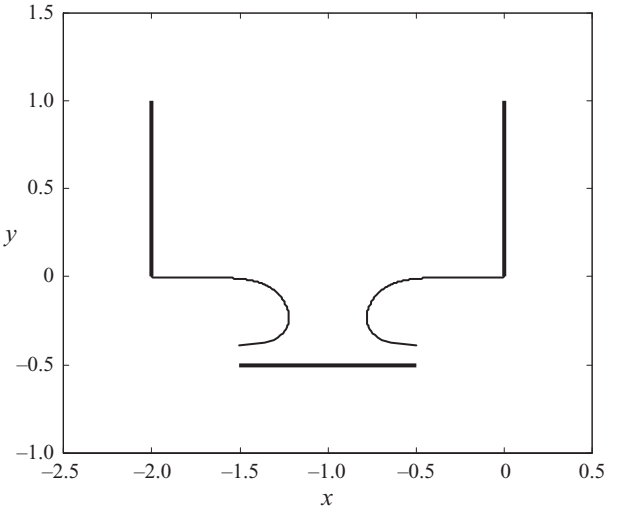


FIGURE 8. Free-surface profiles with 90° stagnation points at A, A' for $H = 0.5$ and $F = 0.1$ ($N = 400$).

For the 90° stagnation points, the numerical process is exactly identical to the one in § 3, where the coefficients a_n in the power series (2.9) are real and can be determined by a collocation Galerkin method, giving again a two-parameter family of solutions. It turns out that such flows exist for 'small' Froude numbers ($F < F_c$, see the 120° case) for values of H larger than the value of H corresponding to the 120° case. For instance, for $F = 0.35$ such solutions exist for $1.01 \leqslant H$, where 1.01 is the corresponding H for the 120° case. An example of a flow with 90° stagnation points is demonstrated in figure 8 for $H = 0.5$ and $F = 0.1$. Such solutions fall into region III of figure 1.

https://doi.org/10.1017/S0022112010001291 Published online by Cambridge University Press

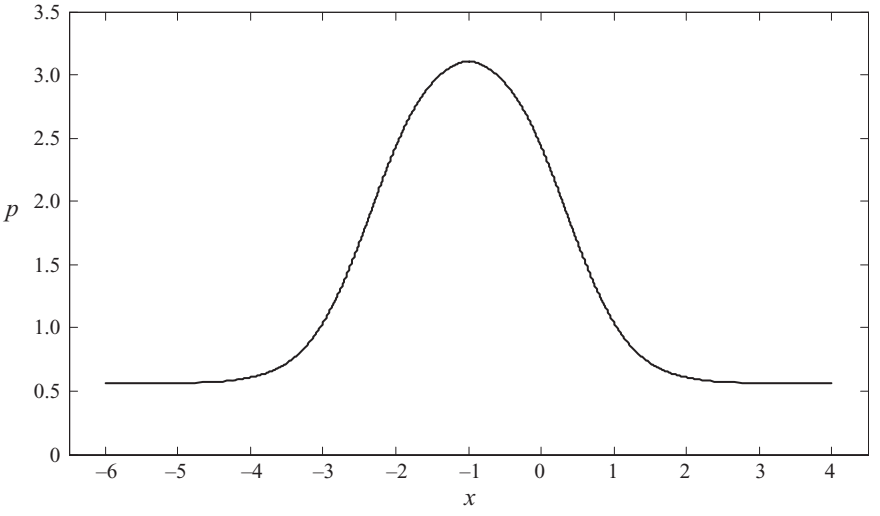


FIGURE 9. Pressure profile along the plate for $H = 1.5$ and $F = 1.5$.

5. Pressure along the plate

Along the horizontal plate, the dimensionless Bernoulli's equation simply reads

$$|\zeta|^2 - \frac{2}{F^2}H + p = |\zeta_A|^2, \tag{5.1}$$

where the pressure p has been non-dimensionalized by $\rho U^2/2$ and $|\zeta_A|$ is the magnitude of the velocity at point A. Figure 9 shows a typical pressure profile along the plate for $H = 1.5$ and $F = 1.5$ (see the case of figure 2*a*).

At the centre of the plate (point C), the pressure is maximum because the velocity is zero. In the case where A is a stagnation point (see § 4), $|\zeta_A|$ becomes identically zero. For a given Froude number F, one can obtain the maximum pressure as a function of height H. In figure 10, we present corresponding results for $F = 0.7$, 1.5 and 5.0. One can clearly observe that the curves exhibit a minimum. This minimum can be explained as follows. For small values of H, the flow has little space between the edge of the pipe and the horizontal plate, as in figure 3. The flow is not affected much by gravity and is close to the no-gravity case considered in the monograph by Milne-Thomson (1996, Example XII.10 and figure 14.8*b*), where an analytical solution was provided. Using our notation, the relationship between H (which is in fact H/W) and the ultimate width $d = D/W$ of the jet in contact with the plate (D being the far-field depth of the stream of fluid on the horizontal plate) reads

$$H = d + \frac{1+d^2}{\pi}\ln\left(\frac{1+d}{1-d}\right). \tag{5.2}$$

In the limit of small H, one finds a constant ratio H/d equal to $1 + 2/\pi$. Let v denote the dimensionless velocity of the uniform flow along the plate (in the far field). Because the mass flux is equal to 1, $d = 1/v$. Neglecting gravity, it follows that $|\zeta_A| = v$. At the centre of the plate (point C), Bernoulli's equation yields approximately

$$p_C \approx |\zeta_A|^2 = \frac{1}{d^2} = \frac{(1+2/\pi)^2}{H^2}. \tag{5.3}$$

https://doi.org/10.1017/S0022112010001291 Published online by Cambridge University Press

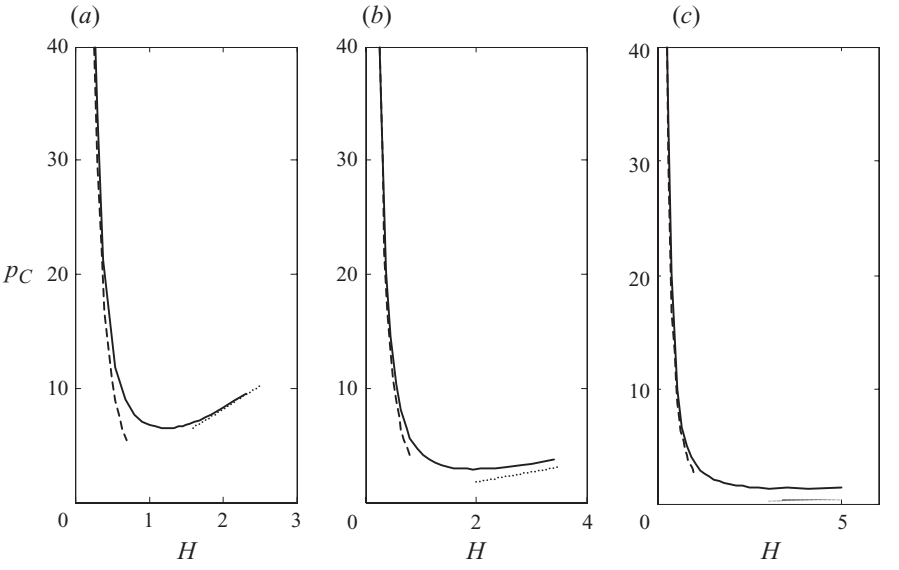


FIGURE 10. Values of the maximum pressure, at the centre C of the plate, as a function of H for (*a*) $F = 0.7$, (*b*) $F = 1.5$ and (*c*) $F = 5.0$ (solid lines). The dashed and dotted lines represent the approximation for small and large values of H, respectively.

The pressure increases quite rapidly as H decreases, as can be seen in figure 10. The behaviour near the minimum is due to the 'squeezing' of the free surfaces discussed in § 3. The two free surfaces tend to 'squeeze' the internal middle flow, thus affecting the pressure exerted at C, which increases despite the increase of the distance H. This phenomenon becomes weaker for higher values of the Froude numbers. Or rather, the minimum occurs at higher values of H (see again § 3). Again, an asymptotic analysis allows us to obtain an estimate for the pressure for large values of H. In that case, the jet experiences a long free fall before hitting the plate. The term containing H in Bernoulli's equation (5.1) is now much larger than the term containing $|\zeta_A|$ so that

$$p_C \approx 2\frac{H}{F^2}. \tag{5.4}$$

The pressure increases linearly as H increases. For large values of the Froude number, the slope $2/F^2$ is quite small, as can be seen in figure 10(*c*).

Let us finally provide a few results with physical dimensions. Taking $U = 2$ m s^{-1}, $H = 15$ m, $W = 4$ m and $\rho = 1000$ kg m^{-3} (with $g = 9.81$ m s^{-2}) yields $F = 0.32$ and, using (5.4),

$$p_C - p_{atm} = 73.575\left(\tfrac{1}{2}\rho U^2\right) = 1.475\,\text{bar}, \tag{5.5}$$

which is a relatively large value. Taking now $U = 2$ m s^{-1}, $H = 1$ m, $W = 4$ m and $\rho = 1000$ kg m^{-3} yields again $F = 0.32$ and, using (5.3),

$$p_C - p_{atm} = 42.856\left(\tfrac{1}{2}\rho U^2\right) = 0.857\,\text{bar}, \tag{5.6}$$

which is still a relatively large value. For this particular value of the Froude number ($F = 0.32$), the minimum for the dimensionless pressure at point C is 17.008. For $U = 2$ m s^{-1}, $W = 4$ m and $\rho = 1000$ kg m^{-3}, it turns out that at the minimum $p_C - p_{atm} = 0.340$ bar.

https://doi.org/10.1017/S0022112010001291 Published online by Cambridge University Press

6. Discussion

The results presented in this paper are based on several assumptions, which we review here. First of all, the flow is assumed to be two-dimensional. A natural extension of this work would be to consider axisymmetric flows. More precisely, one could consider a pipe with a circular cross-section. In the absence of a horizontal plate, this extension was considered by Vanden-Broeck (1991). The main difference with the two-dimensional case is that the rising bubble problem and the falling jet problem must now be solved independently. Another feature of the present calculations is that the pipe is assumed to be vertical. Another natural extension would be to consider inclined pipes. There should not be any technical difficulties. Again this extension was already considered in the absence of a horizontal plate (Lee & Vanden-Broeck 1998). The same can be said about the inclusion of surface tension.

A less obvious extension is that of compressibility. If air is entrained by the jet falling from the pipe, compressible effects can play a role, especially when computing the pressure along the plate. The solutions will depend on an additional dimensionless number, the Mach number. It will be interesting to compare incompressible results with compressible results. Preliminary results can be found in Christodoulides *et al.* (2010).

In Peregrine & Thais (1996), compressibility is taken into account but gravity is neglected. The flows are not computed explicitly. The authors write equations for the conservation of mass and momentum, Bernoulli's equation, the equation of state and a kinematic condition. The extension of their work to our study is not trivial but is worth pursuing in the future. That way one would have a simple model for the impact due to a jet of heavy compressible fluid.

This research has been supported by ANR HEXECO, Project BLAN07-1_192661 and by the 2008 Framework Program for Research, Technological Development and Innovation of the Cyprus Research Promotion Foundation under the Project $A\Sigma TI$/0308(BE)/05.

REFERENCES

Benjamin, T. B. 1968 Gravity currents and related phenomena. *J. Fluid Mech.* **31**, 209–248.

Birkhoff, G. & Carter, D. 1957 Rising plane bubbles. *J. Math. Mech.* **6** (4), 769–779.

Braeunig, J.-P., Brosset, L., Dias, F. & Ghidaglia, J.-M. 2009 Phenomenological study of liquid impacts through 2D compressible two-fluid numerical simulations. In *Proceedings of the Nineteenth International Offshore and Polar Engineering Conference, Osaka, Japan, 21–26 June, 2009*, vol. III, pp. 21–28.

Braeunig, J.-P., Brosset, L., Dias, F., Ghidaglia, J.-M. & Maillard, S. 2010 On the scaling problem for impact pressure caused by sloshing. *Journal of Ship Research* (submitted).

Christodoulides, P. & Dias, F. 2009 Impact of a rising stream on a horizontal plate of finite extent. *J. Fluid Mech.* **621**, 243–258.

Christodoulides, P., Dias, F., Ghidaglia, J.-M. & Kjerland, M. 2010 On the effect of compressibility on the impact of a falling jet. In *Proceedings of the Twentieth International Offshore and Polar Engineering Conference, Beijing, China, 20–25 June, 2010*, vol. III, pp. 53–61.

Couët, B. & Strumolo, G. S. 1987 The effects of surface tension and tube inclination on a two-dimensional rising bubble. *J. Fluid Mech.* **184**, 1–14.

Dias, F. & Tuck, E. O. 1993 A steady breaking wave. *Phys. Fluids* A **5**, 277–279.

Garabedian, P. R. 1957 On steady-state bubbles generated by Taylor instability. *Proc. R. Soc. Lond.* A **241**, 423–431.

https://doi.org/10.1017/S0022112010001291 Published online by Cambridge University Press

Hocking, G. C. 1985 Cusp-like free-surface flows due to a submerged source or sink in the presence of a flat or sloping bottom. *J. Aust. Math. Soc.* B **26**, 470–476.

Hocking, G. C. 1992 Flow from a vertical slot into a layer of finite depth. *Appl. Math. Modelling* **16**, 300–306.

Inogamov, N. A. & Oparin, A. M. 2003 Bubble motion in inclined pipes. *JETP* **97**, 1168–1185.

Korobkin, A. 1995 Impact of two bodies one of which is covered by a thin layer of liquid. *J. Fluid Mech.* **300**, 43–58.

Lee, J. & Vanden-Broeck, J.-M. 1993 Two-dimensional jets falling from funnels and nozzles. *Phys. Fluids* A **5**, 2454–2460.

Lee, J. & Vanden-Broeck, J.-M. 1998 Bubbles rising in an inclined two-dimensional tube and jets falling along a wall. *J. Aust. Math. Soc.* B **39**, 332–349.

Merino, F. 1996 Fluid flow through a vertical slot under gravity. *Appl. Math. Modelling* **20**, 934–939.

Michallet, H., Mathis, C., Maissa, P. & Dias, F. 2001 Flow filling a curved pipe. *Trans. ASME J. Fluids Engng* **123**, 686–691.

Milne-Thomson, L. M. 1996 *Theoretical Hydrodynamics*, 5th edn. Dover.

Modi, V. 1985 Comment on 'Bubbles rising in a tube and jets falling from a nozzle.' *Phys. Fluids* **28** (11), 3432–3433.

Peregrine, D. H. & Kalliadasis, S. 1996 Filling flows, cliff erosion and cleaning flows. *J. Fluid Mech.* **310**, 365–374.

Peregrine, D. H. & Thais, L. 1996 The effect of entrained air in violent water wave impacts. *J. Fluid Mech.* **325**, 377–397.

Tuck, E. O. & Dixon, A. 1989 Surf-skimmer planing hydrodynamics. *J. Fluid Mech.* **205**, 581–592.

Tuck, E. O. & Vanden-Broeck, J.-M. 1984 A cusp-like free-surface flow due to a submerged source or sink. *J. Aust. Math. Soc.* B **25**, 443–450.

Vanden-Broeck, J.-M. 1984 Bubbles rising in a tube and jets falling from a nozzle. *Phys. Fluids* **27** (5), 1090–1093.

Vanden-Broeck, J.-M. 1986 Pointed bubbles rising in a two-dimensional tube. *Phys. Fluids* **29** (5), 1343–1344.

Vanden-Broeck, J.-M. 1991 Axisymmetric jet falling from a vertical nozzle and bubble rising in a tube of circular cross section. *Phys. Fluids* A **3** (2), 258–262.

https://doi.org/10.1017/S0022112010001291 Published online by Cambridge University Press